Few-body nature of Kondo correlated ground states

Maxime Debertolis [1], Serge Florens [1], and Izak Snyman [2]

[1]*Institut Néel, CNRS and Université Grenoble Alpes, F-38042 Grenoble, France*
[2]*Mandelstam Institute for Theoretical Physics, School of Physics, University of the Witwatersrand, Johannesburg, South Africa*

The quenching of degenerate impurity states in metals generally induces a long-range correlated quantum state known as the Kondo screening cloud. While a macroscopic number of particles clearly take part in forming this extended structure, assessing the number of truly entangled degrees of freedom requires a careful analysis of the relevant many-body wave function. For this purpose, we examine the natural single-particle orbitals that are eigenstates of the single-particle density (correlation) matrix for the ground state of two quantum impurity problems: the interacting resonant level model (IRLM) and the single impurity Anderson model (SIAM). As a simple and general probe for few-body versus many-body character we consider the rate of exponential decay of the correlation matrix eigenvalues towards inactive (fully empty or filled) orbitals. We find that this rate remains large in the physically most relevant region of parameter space, implying a few-body character. Genuine many-body correlations emerge only when the Kondo temperature becomes exponentially small, for instance near a quantum critical point. In addition, we demonstrate that a simple numerical diagonalization of the few-body problem restricted to the Fock space of the most correlated orbitals converges exponentially fast with respect to the number of orbitals, to the true ground state of the IRLM. We also show that finite-size effects drastically affect the correlation spectrum, shedding light on an apparent paradox arising from previous studies on short chains.

I. INTRODUCTION

Strongly interacting quantum many-body systems constitute one of the most challenging problems in physics. The combination of a macroscopic number of particles with interactions that are relevant in the renormalization sense puts paid to strategies involving the most commonly used tools of quantum mechanics (perturbation theory, exact diagonalization). Over the past decades, advanced numerical methods have been tailored to reliably extract physical information of interacting fermion models, from the numerical renormalization group (NRG) [1] and density-matrix renormalization group [2] in low dimensions, to continuous time quantum Monte Carlo simulations [3] within the dynamical mean-field theory [4] for higher-connectivity lattices. While answering many physical questions, these methods have not yet fully characterized the link between strong correlations and physical complexity for generic quantum many-body systems.

Some classes of problems that are insurmountable by brute force can be tackled due to a hidden simplicity of the physically relevant states (e.g., ground and low-lying thermal states). Indeed, diagnostic tools such as entanglement measures [5] have shown that the density-matrix renormalization group [6–9] owes its success to the matrix-product state structure of ground states of locally interacting one-dimensional lattices. Insights about entanglement between spatially distinct regions have subsequently led to a deep understanding of the matrix and tensor product state structure of translationally invariant low-dimensional interacting ground states. The conceptual understanding of inhomoge-

neous systems is less complete, as attested to by the ongoing work on many-body localization [10]. A simple starting point for studying nonuniform many-body states is the class of systems known as quantum impurity models [11,12]: while strong interactions are limited to a few local sites, scattering from electronic reservoirs generates complex quantum states showing long-range spatial entanglement, dubbed the Kondo screening cloud [13]. The question of quantifying the amount of correlations contained in such a nonlocal many-body impurity state has not yet been addressed exhaustively [14–16]. In this article, we answer the question "How many of the particles in the Kondo cloud are correlated with each other or with the impurity in the quantum many-body sense?"

Given the central position that the Kondo problem occupies in many-body physics, it may seem that the answer is obvious: many electrons become correlated. After all, the Kondo screening cloud is typically much larger than the Fermi wavelength and thus encompasses many conduction electrons. However, recent studies have come to a different and seemingly paradoxical conclusion [17,18]. These works considered the one-body density matrix (also called the correlation matrix) [19–21] of the Kondo problem. Its eigenvectors define an optimal set of single-particle orbitals that are commonly referred to as "natural orbitals" in the quantum chemistry literature [22]. The associated eigenvalues are ground-state occupation numbers for the natural orbitals. If an occupation number is close to zero or one, i.e., nearly empty of filled, the corresponding orbital is not involved in many-body correlations and is therefore said to be inactive. The remaining orbitals are called active and host correlated particles. One

study [18] found that there is a single active orbital that is "solely responsible for screening the impurity spin in both the weak and strong Kondo coupling regime," and that the resulting singlet is disentangled from the rest of the system. The authors of another study [17] similarly report that they have identified "a dominant single particle wave function that is entangled to the impurity forming a singlet that is, to a great extent, practically disentangled from the rest of the conduction electrons." We will show that this proposed single-correlated-orbital picture at weak coupling is purely a finite-size effect (here "weak coupling" means a small exchange interaction, so that the Kondo temperature is exponentially low). Indeed, in the works quoted, systems consisting of at most a few hundred real-space lattice sites were studied. However, the Kondo length becomes quickly larger than this system size when the dimensionless Kondo coupling is reduced to values below unity. When this happens, Kondo correlations cannot fully develop, and many-body effects are dramatically reduced compared with the thermodynamic limit. Clearly, a systematic characterization of the active space of Kondo-correlated systems in the thermodynamic limit is still lacking, and this will be one important goal of our study. We point out that the question we are asking concerns how to express microscopically the ground state of the system in terms of the complete set of *bare* degrees of freedom, used to define the model. It is of course well known that the *effective* description of excitations at energies sufficiently smaller than the Kondo temperature is that of a Fermi liquid.

We have devised the following method to determine the number of particles taking part in ground-state correlations: We use the NRG to calculate the correlation matrix of a fermionic quantum impurity model. We are particularly interested models that display Kondo correlations. The Wilson grid discretization [12] employed by NRG allows us to study systems with a real-space size that grows exponentially with the dimension of the single-particle Hilbert space. We are thus able to obtain results for the correlation matrix that are converged to the thermodynamic limit. We then use the eigenorbitals of the correlation matrix to construct a trial state containing M active orbitals on top of an uncorrelated Fermi sea. At half filling, minimizing the energy expectation value of the trial state is equivalent to exactly diagonalizing an $M/2$-particle problem in the subspace of active orbitals. The resulting variational energy is compared with the true ground-state energy (very accurately calculated with NRG). If the energy difference is much less than the Kondo temperature, then the trial state is an accurate approximation of the true ground state. When this is the case, we conclude that at most M orbitals ($M/2$ particles) take part in correlations.

We have carried out the above procedure for the interacting resonant-level model (IRLM) that displays *bona fide* Kondo correlations in its charge sector. What we find is surprising: while the picture of a single orbital screening the impurity (advocated in Refs. [17,18]) does not apply in general, neither does the pessimistic view that Kondo correlations involve a macroscopic number of electrons within the large screening cloud. For a realistic Kondo temperature of 10^{-3} times the ultraviolet scale set by the Fermi energy, we find that a trial state with only seven correlated particles approximates the ground-state energy to an accuracy of 1% of the Kondo temperature.

Only when one reaches unrealistic regimes where the Kondo temperature becomes exponentially small does the number of correlated particles in the ground state increase beyond a handful, making impractical a description in terms of natural orbitals. This observation suggests that Fermi-liquid ground states of quantum impurity models in the thermodynamic limit are for practical purposes few-body in nature, thus neither single-body nor many-body, once reformulated in the optimal space of natural orbitals.

An important question concerns whether these results are a general feature of Kondo physics or specific to the IRLM. Arguably, mapping the IRLM to the anisotropic Kondo model might yield a more correlated state than the IRLM ground state. Indeed since IRLM fermions are nonlinear and nonpolynomial functions of the bare fermions of the Kondo model, a few-body correlated IRLM ground state might translate into a truly many-body correlated ground state in the Kondo representation. For instance, the Toulouse point of the Kondo model is certainly nontrivial in the original Kondo framework, while it involves completely free fermions on the IRLM side. We have therefore also studied the Anderson impurity model (SIAM), which displays Kondo correlations in its spin sector. Our study of the SIAM again reveals an exponential decay of the natural orbitals to full occupancy or vacancy for any finite Kondo temperature. Our conclusions are therefore not specific to the IRLM and pertain to other quantum impurity models displaying a Fermi-liquid ground state.

The rest of this article is structured as follows: In Sec. II we introduce the IRLM and discuss its equivalence to the single-channel Kondo model. We also review general properties of the correlation matrix for quantum impurity models. In Sec. III, we examine numerical results for the correlation matrix spectrum, using systematic NRG calculations. Special attention is paid to finite-size effects (extra technical details are given in several Appendixes). In Sec. IV, we propose a few-body ansatz based on natural orbitals, which shows exponential convergence to the numerically exact multiparticle wave function describing our NRG results. Section VI contains our results for the correlation matrix of the SIAM, which shows that our conclusions are not specific to the IRLM. Section VI summarizes our main findings and identifies promising directions for future research.

II. GENERALITIES ON THE CORRELATION MATRIX

A simple setting to probe Kondo correlated states is the interacting resonant-level model [23] (IRLM):

$$\mathcal{H} = U\left(d^\dagger d - \frac{1}{2}\right)\left(c_0^\dagger c_0 - \frac{1}{2}\right) + V(d^\dagger c_0 + c_0^\dagger d)$$
$$+ \sum_{i=1}^{N-2} t_i(c_i^\dagger c_{i-1} + c_{i-1}^\dagger c_i), \tag{1}$$

involving spinless fermions on a tight-binding chain of N sites (including the d level as site $i = -1$). Both the Coulomb interaction U and tunneling V couple the resonant level $d^\dagger$ to the local orbital $c_0^\dagger$ at the start of the chain. Despite the absence of spin degrees of freedom, the IRLM can be mapped onto the spin-anisotropic Kondo model [24–26]. The mapping is exact for energy scales below the ultraviolet scale set by the

Fermi energy measured from the bottom of the band, provided the Kondo coupling times the density of states is sufficiently small, i.e., one is in the universal Kondo regime. The equivalence relies on spin-charge separation in the Kondo model, with only spin-density fluctuations coupling to the magnetic impurity. This subsystem is then bozonized and refermionized in terms of spinless fermions. The procedure was first outlined in Ref. [27]. For a recent review, including careful bookkeeping of phases generated by fermion exchange, see for instance Ref. [28]. This equivalence has been used in the past to study some delicate facets of the Kondo problem with high accuracy, for instance quench dynamics [29]. In the present context, the spinless nature of the IRLM facilitates the bookkeeping that is necessary to compute accurately the correlation matrix.

To introduce the correlation matrix, it is helpful to first consider the properties of uncorrelated fermionic states. These can be viewed as single Slater determinants, characterized by a set of one-particle orbitals $q_n^\dagger$ that are each either filled or empty. The orbitals are linear combinations of the physical orbitals $c_i^\dagger$ used to construct the Hamiltonian, e.g., the lattice site basis, $q_n^\dagger = \sum_i U_{ni} c_i^\dagger$. Introducing the correlation matrix matrix of the physical orbitals $Q_{ij} = \langle c_i^\dagger c_j \rangle$, it is clear that for a Slater determinant one obtains $\sum_{ij} U_{mi} U_{ni}^* Q_{ij} = \langle q_m^\dagger q_n \rangle = \lambda_n \delta_{n,m}$ with $\lambda_n = 0$ or 1, depending whether orbital $q_n^\dagger$ is empty or filled. Note that $\hat{Q}$ is proportional to the one-particle reduced density matrix. Recent studies have used the correlation matrix as a tool to study quantum impurity problems [18–20]. For a general many-body state, the eigenvalues λ_n of the correlation matrix $\hat{Q}$ define occupancies between zero and one. The number of eigenvalues significantly different from zero or one provides a sensitive measure of correlations, while the associated eigenvectors of $\hat{Q}$ define the single-particle basis in which correlations are most economically represented [19]. It is worth pointing out that many NRG studies of impurity models focus on observables associated with the impurity degree of freedom only. The $N \times N$ matrix elements $Q_{i,j} = \langle c_i^\dagger c_j \rangle$ (where i, $j \in \{-1, 0, \ldots, N-2\}$ and $c_{-1} \equiv d$) involve observables in the environment ($i, j > -1$) and observables that are hybridized between the impurity and the environment ($i = -1, j > -1$; $j = -1, i > -1$). Calculating $\hat{Q}$ using NRG is therefore more involved than the standard NRG analysis of impurity problems.

Let us focus now on the general properties of the correlation matrix $\hat{Q}$. Clearly, its eigenvalues λ_n are independent of the choice of one-particle orbitals used in its definition. Since the eigenvalues $\lambda_n = \langle q_n^\dagger q_n \rangle$ correspond to occupancies of the natural orbitals, they belong to the interval [0,1]. As mentioned before, the eigenvalues are either zero or one for a Slater determinant, and their departure from these trivial values signal that the associated orbitals participate in quantum many-body correlations. As a simple example, consider the Bell-like state:

$$|\Psi\rangle = \frac{1}{\sqrt{2}}(c_i^\dagger c_j^\dagger + c_k^\dagger c_l^\dagger)|\Phi\rangle, \tag{2}$$

with $|\Phi\rangle$ being a Slater determinant that does not involve orbitals i, j, k, and l (considered distinct from each other). It is easy to check that, for this state, $\hat{Q}$ has four eigen-

values different from zero or one, that are all equal to 1/2. The IRLM Hamiltonian (1) manifests particle-hole symmetry $\mathcal{H} = P^\dagger H P$, where P is the unitary and Hermitian particle-hole conjugation operator:

$$P = \prod_{i=0}^{\frac{N}{2}-1} (c_{2i-1} - c_{2i-1}^\dagger)(c_{2i} + c_{2i}^\dagger), \tag{3}$$

acting as $P^\dagger c_i P = (-1)^i c_i^\dagger$ and $P|0\rangle = c_{-1}^\dagger c_0^\dagger \ldots c_{N-2}^\dagger |0\rangle$. Since $P^2 = 1$, the eigenvalues of P are ± 1, and we have $Q_{ij} = \delta_{ij} - (-1)^{i+j} Q_{ji}$, thus the diagonal entries of $\hat{Q}$ are all equal to 1/2. Furthermore, the matrix elements of the Hamiltonian $\mathcal{H}$ are all real in the Fock-space basis built from $c_i^\dagger$ operators and hence the expansion coefficients of the eigenstates of $\mathcal{H}$ in this basis are real, too. This implies $Q_{ij} = Q_{ji}$, and from the particle-hole symmetry of $\hat{Q}$, we conclude that $Q_{ij} = 0$ for $i + j$ even and $i \neq j$. Owing to particle-hole symmetry the eigenvalues of $\hat{Q}$ then come in pairs $1/2 \pm r$.

III. STUDY OF THE INTERACTING RESONANT-LEVEL MODEL CORRELATION SPECTRUM

The relatively low computational cost to implement NRG for the IRLM makes it possible to track with high accuracy the flow of the N^2 operators $c_i^\dagger c_j$ needed for calculating $\hat{Q}$ with modest computational resources, provided the block-diagonal structure imposed by particle-number conservation is exploited to keep matrix dimensions manageable. Aiming to resolve $\hat{Q}$ eigenvalues that are exponentially small, we calculate the elements of $\hat{Q}$ to a very high precision, allowing up to thousands of kept states after truncation (see Appendix A for a detailed study of the convergence). The NRG implementation is based on the hopping amplitudes along the Wilson chain [12]:

$$t_j = \frac{(1 + \Lambda^{-1})(1 - \Lambda^{-j-1})}{2\sqrt{1 - \Lambda^{-2j-1}}\sqrt{1 - \Lambda^{-2j-3}}} \Lambda^{-j/2} D, \tag{4}$$

so that $D = 1$ sets the half-bandwidth of the bath and also our Fermi energy. We present here calculations for the Wilson parameter $\Lambda = 1.5$ (a more systematic study is presented in Appendix A), tunneling $V = 0.15D$ and up to $N = 180$ sites. The lowest energy at play is thus of the order $\Lambda^{-N/2} D \simeq 10^{-16} D$, ensuring convergence to the ground state for all practical purposes.

Figure 1 displays the full eigenspectrum of $\hat{Q}$, showing on the left side $1 - \lambda_n$ for $1/2 < \lambda < 1$, and on the right side λ_n for $0 < \lambda_n < 1/2$, so that particle-hole symmetry becomes apparent. Note that the eigenvalue index n runs from $-N/2$ to $N/2$, excluding $n = 0$, in order to display more clearly the particle-hole conjugation. The general behavior of the particle-hole symmetrized spectrum is as follows. There is an approximate fourfold degeneracy of the highest eigenvalue $\lambda_{\max} \equiv \lambda_1 = 1 - \lambda_{-1}$, indicating Bell-like entanglement between the four most correlated orbitals $q_{-1}^\dagger, q_{-2}^\dagger, q_1^\dagger, q_2^\dagger$ (from our chosen convention, the index n is centered around those most correlated orbitals). This is related to the fact that, at negative U, the impurity orbital and the first energy shell tend to be either both filled or both empty due to Coulomb attraction, and similarly, at positive U, if the impurity orbital is filled,
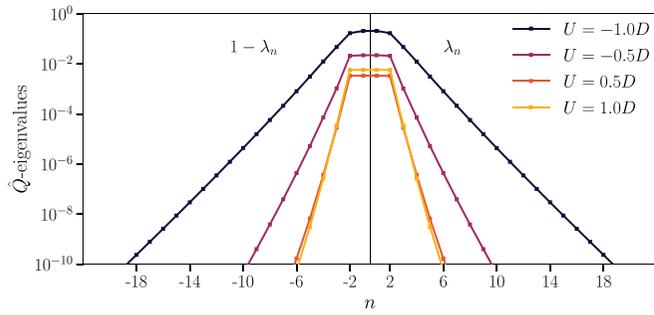
FIG. 1. (top panel) Spectrum of $\hat{Q}$ for the IRLM at various values of interaction U for $V = 0.15$, in units of the half bandwidth $D = 1$. The right side shows eigenvalues $0 < \lambda_n < 1/2$, while the left side shows $1 - \lambda_n$ for $1/2 < \lambda_n < 1$, thus exhibiting particle-hole symmetry explicitly. Apart from four strongly correlated orbitals on the plateau (around which the horizontal index n is centered), the rest of the eigenvalues decay exponentially fast towards either the empty and filled occupancies. In Appendix A it is demonstrated that these results are converged to the continuum and thermodynamic limit $N \to \infty$, $\Lambda \to 1$.

the first energy shell tends to be empty, and vice versa. The other eigenvalues decay exponentially, $\lambda_n \simeq A e^{-xn}$ for $n > 2$ and $\lambda_n \simeq 1 - A e^{+xn}$ for $n < -2$, with a decay rate x that depends on interaction strength. We show in Appendix A that this exponential decay is not an artifact of the Wilson chain and is robust in the continuum limit $\Lambda \to 1$. This behavior of the $\hat{Q}$ eigenvalues has previously been observed in studies of impurity models discretized on regular real-space lattices [18–20]. We emphasize that the Kondo regime corresponds to $U < 0$ in the IRLM, and indeed the slower decay of the $\hat{Q}$ eigenvalues in Fig. 1 attests that this regime is more correlated than for $U > 0$.

The behavior of $\lambda_{\max}$, the maximum eigenvalue of $\hat{Q}$ in the range $[0, 1/2]$, is displayed as a function of interaction U in Fig. 2, showing that it remains small for all $U > 0$ (this is the weakly correlated sector of the IRLM), vanishes at $U = 0$ (the ground state is a Slater determinant, so that all eigenvalues are trivial), and increases sharply only for $-1.3 < U < -1.0$ due to the approach to the IRLM quantum critical point $U_c = 1.3$ where the Kondo temperature vanishes. Our key observation is that the decay rate x of the $\hat{Q}$ eigenvalues drops to small values only when the Kondo temperature becomes exponentially small, seemingly with a linear vanishing as $|U - U_c|$ (see middle panel), as also shown by the slow inverse logarithmic decrease of x as a function of Kondo temperature (see bottom panel of Fig. 2). Thus, only the quantum critical regime corresponds to a true many-body state as opposed to a few correlated particles on top of an uncorrelated Fermi sea. Larger negative $U < -1.3$ leads to a discontinuous transition to a phase where particle-hole symmetry is broken (corresponding to the ferromagnetic phase of the Kondo Hamiltonian), involving clearly less correlations due to a jump of the decay rate x to finite values.

Our results are seemingly inconsistent with results for the Kondo model reported in Refs. [17,18]. According to these studies, x should become large close to the phase transition, whereas we find that it vanishes. To shed light on the apparent
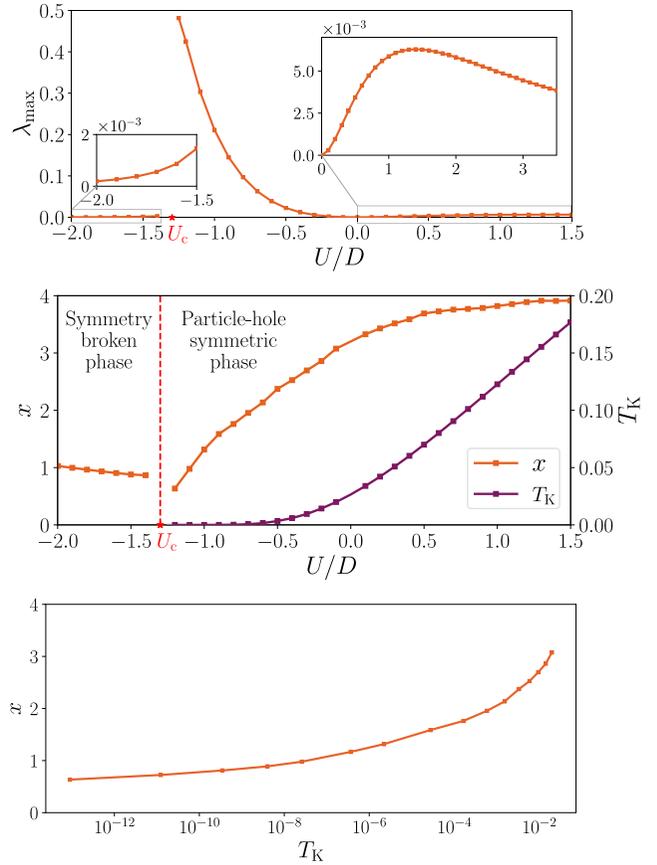
FIG. 2. (top panel) Maximum $\hat{Q}$ eigenvalue $\lambda_{\max}$ as a function of interaction U. (middle panel) Decay rate x of the $\hat{Q}$ eigenvalue (upper curve) and Kondo temperature T_K (lower curve) versus U. Only the quantum critical regime near $U_c \simeq -1.3$ is strongly correlated, since the Q eigenvalues show both a slow decay ($x < 1$) and an enhanced $\lambda_{\max} \simeq 0.5$. (bottom panel) Decay rate x replotted as a function of Kondo temperature T_k, showing a slow inverse logarithmic decrease of x when T_k vanishes at the IRLM quantum critical point.

paradox, we show in Fig. 3 the spectrum of $\hat{Q}$ as a function of the number N of Wilson chain sites. The real-space system size is $\Lambda^{N/2}$. Here we used $\Lambda = 2.25$ and picked a point $U = -1.2$ close to the critical point. For this choice, the Kondo length has the astronomically large value $1/T_K = 10^{13}$, which matches the system size when $N = 75$. (In Appendix C we explain how the Kondo temperature T_K is calculated.) For N significantly smaller than 75, we see very quick exponential decay of the spectrum, corresponding to large x and a ground state with few correlated particles. However, when N increases beyond 75, the decay rate x soon saturates to a small value, so that a large number of correlated particles participate in the true ground state in the thermodynamic limit. These finite-size artifacts explain the results reported in Refs. [17,18] where real-space lattices with at most a few hundred sites were studied, leading to system sizes of the order of a hundred times the Fermi wavelength. The exponentially diverging Kondo length reaches this order of magnitude long before the weak-coupling regime in the vicinity of the critical point is entered. In terms of IRLM
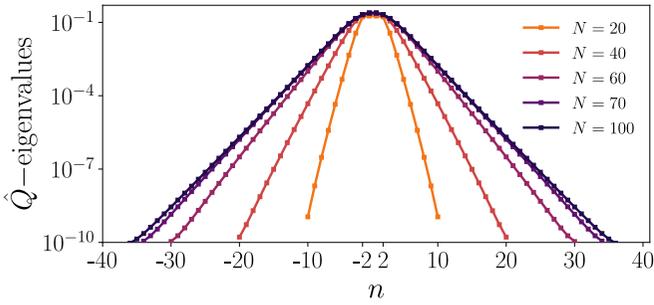
FIG. 3. Finite-size scaling of the $\hat{Q}$-matrix spectrum for $U = -1.2$ near the quantum critical point, for various system sizes N. To reach the exponentially long Kondo length $1/T_K = 10^{13}$, a slightly larger discretization parameter $\Lambda = 2.25$ was used. The corresponding real-space system size $\Lambda^{N/2}$ equals the Kondo length when $N = 75$, as seen by the convergence to the thermodynamic limit for $N > 80$. Smaller systems are plagued by finite-size effects that preempt the full formation of the Kondo state and show a very rapid decay of the $\hat{Q}$ eigenvalues.

FIG. 4. (main panel) Decay rate x versus d-level on-site energy ϵ_d, at $U = -1.0$, $V = 0.15$, and discretization parameter $\Lambda = 1.5$. The corresponding Kondo temperature is $T_K = 1.87 \times 10^{-6}$. Correlations are clearly weakened (x increases) when breaking the charge degeneracy of the d level as ϵ_d increases. Inset shows ground-state d level occupancy $\langle d^\dagger d \rangle$ versus d-level on-site energy ϵ_d, for the same parameters as used in the main panel.

parameters, a system size between 10^2 and 10^3 times the Fermi wavelength prevents a fully correlated ground state from forming for $U < -0.5$ and leads to a severe overestimate of the decay rate x close to the critical point. Figure 3 clearly establishes that correlations increase when the Kondo cloud becomes more extended, in agreement with intuition.

A standard method for probing Kondo correlations is to perturb the system at the Kondo scale and to see the effect this has on observables. For instance, a biasing potential $\epsilon_d d^\dagger d$ in the IRLM, corresponding to a Zeeman splitting between the spin-up and spin-down states of the magnetic impurity in the Kondo model, prevents formation of the Kondo singlet. The occupancy $\langle d^\dagger d \rangle$ (or equivalently the impurity magnetization) reveals significant symmetry breaking when ϵ_d reaches the Kondo scale. It is intuitively clear that the symmetry breaking in the ground state is a sign of reduced correlations, but the observable $\langle d^\dagger d \rangle$ does not directly measure this—one can clearly modify the degree of correlations in the ground state without changing $\langle d^\dagger d \rangle$ at half filling ($\epsilon_d = 0$) when U is changed. The spectrum of $\hat{Q}$, on the other hand, directly measures correlations. In Fig. 4 we plot the decay rate x of the $\hat{Q}$ eigenvalues as a function of ϵ_d. The calculation was performed for $U = -1.0$ and $V = 0.15$, which corresponds to $T_K = 1.87 \times 10^{-6}$. We used $\Lambda = 1.5$ which yields a decay rate x that is converged to the $N \to \infty$, $\Lambda \to 1$ limit. For comparison, we also plot $\langle d^\dagger d \rangle$ versus ϵ_d in the inset of Fig. 4. We see that x starts changing from its unperturbed value when ϵ_d exceeds the Kondo temperature. As ϵ_d increases further, x increases monotonically, indicating that fewer and fewer correlated particles are present, the more severely singlet formation is prevented. In this way, the $\hat{Q}$ matrix spectrum proves the picture suggested by the d-level occupancy $\langle d^\dagger d \rangle$.

We now examine the spatial dispersion (along the Wilson chain) of the $\hat{Q}$-matrix orbitals $q_n^\dagger = \sum_i U_{ni} c_i^\dagger$ by plotting the absolute value $|U_{ni}|$ of the eigenvectors obtained from the diagonalization of the matrix Q_{ij} (this also displays particle-hole symmetry more clearly). Figure 5 shows how correlations spread along the system for four values of the interaction U. It is clear from Fig. 5 that all the natural orbitals

are highly nonlocal and carry information mostly forward along the chain. The most correlated orbitals ($n = 1$ and $n = -1$) are predominantly localized near the impurity (site $i = -1$), as expected from the short range of the interaction, but develop also long tails that extend to large distances. For $U > 0$, the spatial structure of correlated orbitals is fairly insensitive to the interaction strength, showing that this regime remains weakly correlated. In contrast, for negative values of the interaction, as we go closer to the quantum critical point $U_c = -1.3$, correlated orbitals become more delocalized, due to the divergence of the Kondo length. In addition, more and more orbitals become entangled, due to the slower decay of the eigenvalues λ_n in Fig. 1.
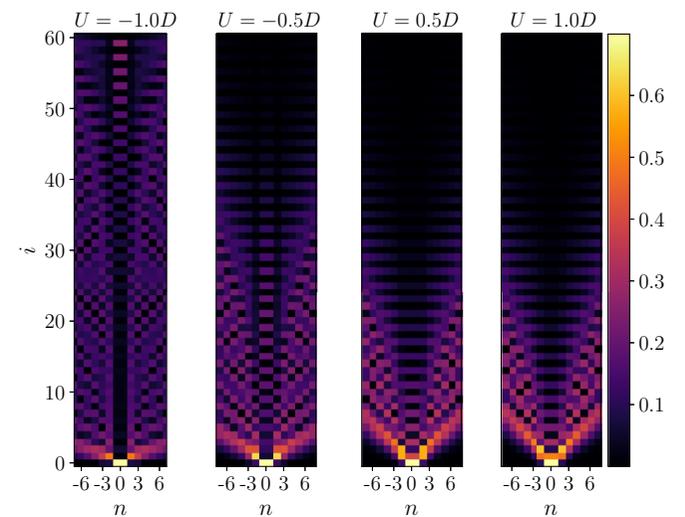
FIG. 5. Spatial dispersion of the 14 most correlated orbitals $q_n^\dagger$ ($n = -7, \dots, 7$) along the Wilson chain (sites $i = -1, \dots, 60$), given by the absolute value of eigenvectors $|U_{ni}|$. The development of Kondo correlations for $U < 0$ is evinced by the long spatial tails, especially at $U = -1.0$, while little is changed in the spatial profile for the weakly correlated regime $U > 0$.

IV. FEW-BODY ANSATZ FROM NATURAL ORBITALS

Equipped with this construction of the natural orbitals of the $\hat{Q}$ matrix, we establish our most surprising finding, namely, that the ground state of the IRLM is few-body in nature for realistic (i.e., nonexponentially vanishing) Kondo temperatures. This result is clearly suggested by the exponential decay of the $\hat{Q}$ matrix eigenvalues in Fig. 1. Since most of the eigenvalues λ_n are exponentially close to either zero or one, it seems a good approximation to assume that their associated orbitals are exactly uncorrelated, keeping a core of M truly correlated orbitals within the ground-state wave function (those orbitals correspond to the $M\lambda_n$ eigenvalues that are closest to $1/2$, and we choose M to be even, which allows for a correlated sector that is exactly half filled). Specifically, half of the $N - M$ uncorrelated orbitals (those that have their eigenvalues closest to 1) will be frozen and described by a Slater determinant

$$|\Psi_0\rangle = \prod_{m=-\frac{N}{2}}^{-\frac{M}{2}-1} q_m^\dagger |0\rangle$$

in the eigenorbitals of the correlation matrix computed by NRG. The other half of the uncorrelated orbitals (those with $\hat{Q}$ eigenvalues closest to 0) are taken as empty. We therefore write the full wave function as follows:

$$|\Psi_{\text{few}}\rangle = \sum_{\{N_n\}} \Psi\left(N_{-\frac{M}{2}}, \ldots, N_{\frac{M}{2}}\right) \prod_{n=-\frac{M}{2}}^{\frac{M}{2}} [q_n^\dagger]^{N_n} |\Psi_0\rangle, \quad (5)$$

with $N_n = 0, 1$ being the occupancy of correlated orbital $q_n^\dagger$, the summation restricted to occupations such that $\sum_{n=-M/2}^{M/2} N_n = M/2$, and $\Psi(N_{-\frac{M}{2}}, \ldots, N_{\frac{M}{2}})$ being the complete few-body wave function in the correlated subspace. Note that the total set of $\hat{Q}$ orbitals runs with index $n = -N/2, \ldots, N/2$, as in Fig. 1, and that the index $n = 0$ is excluded in the above expression. We stress that such an ansatz is very common in quantum chemistry, where an active space (also dubbed the correlated sector) is used to select the most important chemical degrees of freedom [22].

The Hamiltonian can be reexpressed within the $q_n^\dagger$ orbitals, and then exactly divided into three pieces: $\mathcal{H} = \mathcal{H}_{\text{corr}} + \mathcal{H}_{\text{uncorr}} + \mathcal{H}_{\text{mix}}$, depending on whether the indices n act only within the correlated sector (first term), or only within the uncorrelated sector (second term), or mix both sectors (third term). Minimizing $\langle\Psi_{\text{few}}|\mathcal{H}|\Psi_{\text{few}}\rangle$ with respect to the few-body wave function $\Psi(N_{-\frac{M}{2}}, \ldots, N_{\frac{M}{2}})$ yields a variational energy equal to the ground-state energy of the few-body Hamiltonian $\mathcal{H}_{\text{few}} = \mathcal{H}_{\text{corr}} + \Pi(\mathcal{H}_{\text{uncorr}} + \mathcal{H}_{\text{mix}})\Pi^\dagger$, which acts on states in which electrons occupy correlated orbitals only, with $\Pi = \prod_{m=-\frac{N}{2}}^{-\frac{M}{2}-1} q_m$. Within the Fock space constructed from correlated orbitals only, $\Pi\mathcal{H}_{\text{uncorr}}\Pi^\dagger$ is a real number, while $\Pi\mathcal{H}_{\text{mix}}\Pi^\dagger$ is a quadratic operator (see Appendix B for details). The optimal wave function $\Psi(N_{-\frac{M}{2}}, \ldots, N_{\frac{M}{2}})$ can be found by exact diagonalization of the few-body Hamiltonian $\mathcal{H}_{\text{few}}$, which we have done for increasing values of M.

The only relevant parameter of the few-body approximation is the number M of kept correlated orbitals. Obviously,
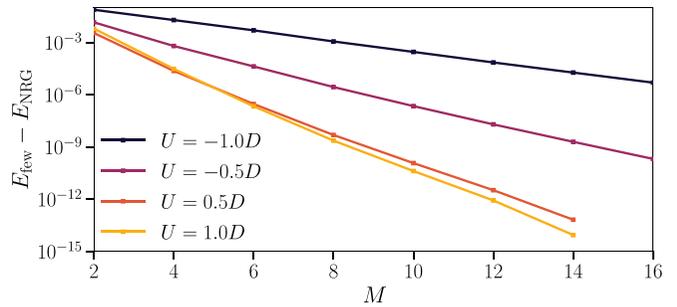
FIG. 6. Difference between the ground-state energy E_{few} computed with the few-body wave function (5) and the numerically exact energy E_{NRG} obtained from NRG, as a function of the number of correlated orbitals.

the limit $M \to N$ would lead to the exact wave function. We stress that all computations at finite M are done in the thermodynamic limit, since the $N - M$ uncorrelated orbitals are fully accounted for in our ansatz (5). These uncorrelated orbitals actually constitute a major part of the total energy, despite being evaluated in a single-particle picture. The difference between the computed few-body energy $E_{\text{few}} = \langle\Psi_{\text{few}}|\mathcal{H}|\Psi_{\text{few}}\rangle$ at fixed M and the many-body ground-state energy E_{NRG} obtained from the converged NRG simulations is shown in Fig. 6. We find an exponential convergence of the few-body energy as a function of the number M of correlated orbitals, as anticipated from the structure of the $\hat{Q}$-matrix spectrum. Note that, for the half filling considered here, the number of truly interacting fermions is $M/2$. We see that an accuracy of six digits is obtained for six correlated orbitals (three interacting particles) for all $U > 0$. For $U < 0$, the rate of convergence becomes slower the closer we come to the critical point, consistent with the increase in the number of $\hat{Q}$ eigenvalues that are significantly different from zero or one. However, even at $U = -1.0$, where the Kondo temperature is 1.87×10^{-6}, 20 correlated orbitals (10 interacting particles) would give an accuracy better than 10% of the Kondo temperature. This clearly vindicates our claim that, for practical purposes, the ground state of the Kondo problem is few-body and not many-body in nature, once expressed in the optimal set of natural orbitals. Only exponentially close to a quantum phase transition does a truly many-correlated-particle wave function emerge, as discussed previously for dissipative systems [30].

V. CORRELATION SPECTRUM OF SINGLE IMPURITY ANDERSON MODEL

In this final section, we investigate whether our results extend to other impurity models by investigating the correlation spectrum of the single impurity Anderson model (SIAM). The IRLM and SIAM share the same universal low-energy physics at scales that are small compared with the ultraviolet cutoff, although Kondo correlations pertain to the charge sector of the IRLM and to the spin sector of the SIAM. Does this automatically mean that the ground state of the SIAM (and other models in the same Kondo universality class) is few-body in nature, as long as T_K is finite but sufficiently smaller than the ultraviolet cutoff? The universality of Kondo physics does not settle this question, for the following

reason: The fermionic operators that appear in the IRLM are nonlinear (and nonpolynomial) functions of those appearing in the definition of the anisotropic Kondo Hamiltonian. Our results up to this point show that the Kondo ground state is effectively few-body in nature, when expressed in terms of IRLM fermions, and it remains to be checked whether this is also true in other representations, such as the arguably more fundamental fermions of the SIAM.

To address this question, we investigate the correlation matrix of the single impurity Anderson model (SIAM):

$$\mathcal{H} = U\left(d_\uparrow^\dagger d_\uparrow - \frac{1}{2}\right)\left(d_\downarrow^\dagger d_\downarrow - \frac{1}{2}\right)$$
$$+ V\sum_{\sigma=\uparrow,\downarrow}(d_\sigma^\dagger c_{0,\sigma} + c_{0\sigma}^\dagger d_\sigma)$$
$$+ \sum_{\sigma=\uparrow,\downarrow}\sum_{i=1}^{N-2}t_i(c_{i,\sigma}^\dagger c_{i-1,\sigma} + c_{i-1,\sigma}^\dagger c_{i,\sigma}), \qquad (6)$$

whose effective low-energy description in the strong-interaction limit $U \gg \Gamma = V^2/(2D)$ is the Kondo model, D being the half-bandwidth. Hamiltonian (6) is again discretized on the Wilson chain, and we used particle number as well as spin conservation to optimize the numerical simulations, as the spinfulness of the SIAM fermions doubles the dimensions of the single-particle Hilbert space. Because the ground state is a spin singlet, $\langle c_{i\sigma}^\dagger c_{j\sigma'}\rangle \propto \delta_{\sigma\sigma'}$ and $\langle c_{i\uparrow}^\dagger c_{j\uparrow}\rangle = \langle c_{i\downarrow}^\dagger c_{j\downarrow}\rangle$. Thus there is an extra twofold degeneracy in the correlation matrix spectrum, as compared with the IRLM. The NRG calculation of the correlation matrix demands more computational resources than for the IRLM, but as we show in Appendix A, we succeeded in obtaining well-converged results. As for IRLM, we include the d-level fermions in the operators used to construct the correlation matrix, so that the limit $U = 0$ is strictly uncorrelated.

The top panel of Fig. 7 shows the correlation matrix spectrum, plotted in the same way as for the IRLM in Fig. 1. Beyond a central plateau, that still contains the four eigenvalues furthest from full occupancy or vacancy, we see degenerate pairs $\lambda_{n\uparrow} = \lambda_{n\downarrow}$ that decay exponentially $\lambda_{n\sigma} \sim \exp(-x|n|)$. In the bottom panel of Fig. 7, we show the extracted decay rate x, as a function of the Kondo temperature T_k (the latter is calculated from the magnetic susceptibility of the impurity). We see a finite decay rate even at extremely low Kondo temperatures $\approx 10^{-12}$ of the bandwidth, and our results are consistent with x vanishing at zero Kondo coupling $(U \to \infty)$.

The exponential decay of correlation matrix eigenvalues (natural orbital occupation numbers) to full occupancy or vacancy therefore is not a special feature of the IRLM representation of Kondo physics. Thus, also for the SIAM, the single-particle Hilbert space can be partitioned into an M-dimensional correlated sector and a remainder that is uncorrelated. An ansatz that straightforwardly generalizes (5) can be constructed. Its accuracy is controlled by M, and any desired accuracy can be obtained with an M that remains finite in the thermodynamic limit. Due to the fact that there is an extra degeneracy in the correlation matrix spectrum of the SIAM and also because, for given T_K, the decay rate x is roughly
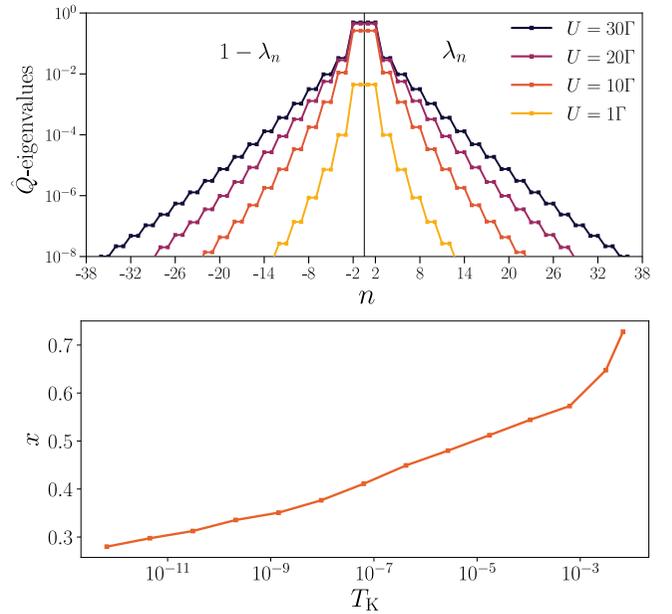
FIG. 7. (top panel) Correlation matrix spectrum for the single impurity Anderson model (SIAM) for various ratios of the onsite interaction U to the hybridization Γ. In all cases $\Gamma = 0.01D$. As in Fig. 1, the right side shows eigenvalues $0 < \lambda_{n\sigma} < 1/2$, while the left side shows $1 - \lambda_{n\sigma}$ for $1/2 < \lambda_{n\sigma} < 1$. Spin degenerate pairs of eigenvalues $\lambda_{n\sigma}$ decay exponentially $\sim \exp(-|n|x)$ to full occupancy or vacancy. (bottom panel) Decay rate x of correlation matrix eigenvalues versus Kondo temperature T_k.

twice smaller for SIAM fermions than for IRLM fermions, a larger M will be required for the same accuracy at a given T_K than in the IRLM. As a practical matter, this limits the range of Kondo couplings for which few-body approximations to the ground state of the SIAM can be found numerically, but, in principle, the SIAM ground state is effectively a few-body correlated state in terms of SIAM fermions, in the same way that the IRLM ground state is few-body in nature, provided T_K is finite.

VI. CONCLUSIONS

We have calculated the correlation matrix of the IRLM and the SIAM, two quantum impurity models that are equivalent to the single-channel Kondo Hamiltonian. Several recent studies have noted that the eigenvalues of the correlation matrix of quantum impurity models often decay exponentially towards full occupation or vacancy [18–20], and our results confirm this observation, provided that the ground state is not quantum critical. We have, however, identified results in the literature about the Kondo model, namely, that the exponential decay rate of correlation matrix eigenvalues becomes large close to the weak-coupling critical point, which are finite-size artifacts. We demonstrated that, in fact, the decay rate tends to zero as the critical point is approached for a macroscopically large electronic bath. Finite-size systems that are smaller than the Kondo length prevent the full development of correlations. We have also investigated the spatial structure of the most

correlated natural orbitals as the critical point is approached and detected clear fingerprints of the Kondo screening cloud.

Our main result presents a general method for determining the effective number of correlated particles (on top of an uncorrelated Fermi sea). This involves using the natural orbital single-particle basis to identify correlated and uncorrelated sectors of Fock space. Owing to the exponential decay of the correlation matrix spectrum to full occupancy or vacancy, the correlated sector can, to a good approximation, be chosen to contain a finite number of particles $M/2$, whereas the uncorrelated sector contains an infinite number of particles within a single Slater determinant in the thermodynamic limit. The full ground state can be reconstructed approximately by solving an effective few-body problem for the particles in the correlated sector. If the reconstructed state has an energy expectation value that differs from the true ground state by an amount that is significantly less than the Kondo temperature, then the reconstructed state is a faithful approximation of the true ground state. By comparing the energy of this reconstructed state to the true ground-state energy, as a function of M, we can thus determine the effective number of correlated particles. Whereas the number of correlated particles diverge at the weak-coupling fixed point ($T_K \to 0$), for realistic Kondo temperatures of $\approx 10^{-3}$ of the Fermi energy, the ground state only hosts around seven correlated particles in the IRLM representation, and a larger but still finite number in the SIAM. The different models host different numbers of correlated particles at the same Kondo temperature because their microscopic degrees of freedom are nontrivially related. We have investigated how this picture is affected when correlations are frustrated, either by finite-size effects or by symmetry-breaking fields. We showed that, as expected, physical cutoffs acting near the Kondo scale are accompanied by a sharp reduction in the number of correlated particles. However, we anticipate that models tuned to criticality, such as the two-channel and two-impurity Kondo models, remain truly many-body in any single-particle basis. Our results open many interesting avenues for research, such as generalizations to other quantum impurity problems or even to disordered lattice models. It would also be interesting to investigate whether this few-body picture is robust for excited or unitarily time-evolved states, a notoriously challenging problem for strongly interacting fermions.

APPENDIX A: CONVERGENCE OF THE SPECTRUM OF $\hat{Q}$ TO THE THERMODYNAMIC LIMIT

The thermodynamic limit of the Wilson chain used in NRG is obtained mathematically by sending the chain length N to infinity and subsequently sending Λ to 1. For the IRLM, this limit describes a one-dimensional conduction band with a constant density of states coupled via hybridization and short-range Coulomb interactions to a resonant level. In practice, numerical calculations are performed at finite N and

$\Lambda > 1$, and also introduce a further regularization parameter N_{kept}, which is the maximum dimension to which fixed particle number sectors of Hilbert space are truncated in each renormalization step. In this section we demonstrate that our numerical results are converge to the thermodynamic limit with respect to these three regularization parameters. We first show in Fig. 8 (top panel) that the $\hat{Q}$-matrix spectrum is indeed well converged for sufficiently long chains. Here, we consider an interaction value $U = -1.2D$ very close to the quantum critical point $U_c = -1.3D$, leading to an exponentially small Kondo temperature of order $T_K/D \simeq \Lambda^{-75/2} \simeq 10^{-13}$, which is estimated from the crossover at $N \simeq 75$ seen in the flow of the lowest eigenvalues of the rescaled Hamiltonian (bottom-right panel in Fig. 8), using the value $\Lambda = 2.25$ for this NRG computation. The same crossover scale is seen for all eigenvalues λ_n (see bottom-left panel in Fig. 8), which are well saturated to their $N = \infty$ limit for $N > 75$. Note however, that eigenvalues λ_n with $n > N/2$ are not defined since the chain is too short to harbor those modes. Longer chains are thus required to obtain such small eigenvalues.

We then investigate the issue of the convergence to the continuum limit $\Lambda \to 1$. In the left panel of Fig. 9, we plot the $\hat{Q}$ spectrum for $U = 0.5$, with $N_{\text{kept}} = 450$ many-body states per block, for various Λ values. The first five eigenvalues are clearly independent of Λ, showing that the exponential falloff is robust in the thermodynamic limit. For the smaller eigenvalues λ_n with $n \geqslant 6$, some departure of the exponential decay is seen for $\Lambda = 1.5$ and $\Lambda = 1.4$. We show in the middle panel of Fig. 9 that this artifact is purely an effect of the truncation error on the exponentially small magnitude of the eigenvalues, that disappears progressively when increasing N_{kept}. Thus, in practice, calculations with $\Lambda = 2$ and $N_{\text{kept}} \simeq 450$ provide good convergence for spinless models, emphasizing that it is not useful to consider λ_n eigenvalues below the machine precision 10^{-16}. We found similar results for other values of the interaction U.

In Sec. V we presented results for the spectrum of the correlation matrix of the single impurity Anderson model. Given the larger single-particle Hilbert space, it is important to make sure that these results are converged with respect to NRG truncation. In the right panel of Fig. 9, we show that this is the case: The evolution of the spectrum of the numerically computed correlation matrix for the SIAM as a function of N_{kept} closely mirrors that of the IRLM (compare with the middle panel of Fig. 9.) We clearly see that the truncation error is pushed closer and closer to full occupancy or vacancy as N_{kept} is increased, and that results are consistent with a spectrum that decays exponentially to full occupancy or vacancy.

APPENDIX B: FEW-BODY DIAGONALIZATION IN THE $\hat{Q}$ EIGENBASIS

We present here some technical details on how to perform an exact diagonalization of an arbitrary nonlocal Hamiltonian, using the eigenvectors of the $\hat{Q}$ matrix as an optimized set of M correlated orbitals $q_n^\dagger$, with $n = -M/2, \ldots, -1, 1, \ldots, M/2$. The orbitals with $-N/2 \leqslant n < -M/2$ are fully occupied, while the orbitals with $M/2 < n \leqslant N/2$ are totally empty. As discussed in the main text, we write
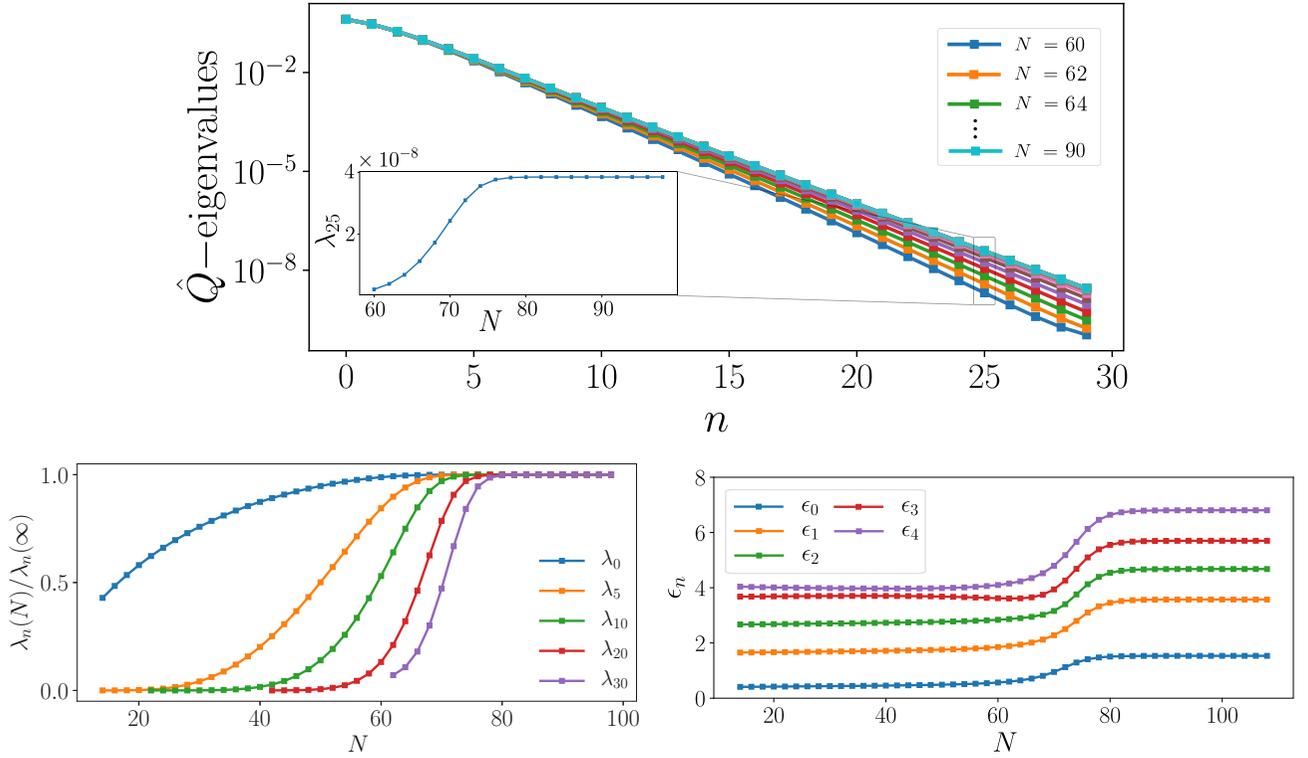
FIG. 8. (top) $\hat{Q}$-matrix spectrum for $U = -1.2D$ near the quantum critical point $U_c = -1.3D$ for various chain lengths N ($\Lambda = 2.25$ here). (bottom left) The same data, plotted as a function of N, showing convergence for $N > 75$. (bottom right) The corresponding flow of the five lowest eigenvalues of the rescaled Hamiltonian. Both the $\hat{Q}$ eigenvalues $\lambda_n(N)$ and the H eigenvalues $\epsilon_n(N)$ show a crossover to the Kondo fixed point at a scale $N \gtrsim 75$, corresponding to $T_K/D \simeq 2.25^{-75/2} \simeq 10^{-13}$.

the full wave function as follows:

$$|\Psi_{\text{few}}\rangle = \sum_{\{N_n=0,1\}} \Psi\left(N_{-\frac{M}{2}}, \ldots, N_{\frac{M}{2}}\right) \prod_{n=-\frac{M}{2}}^{\frac{M}{2}} [q_n^\dagger]^{N_n} |\Psi_0\rangle,$$

$$|\Psi_0\rangle = \prod_{m=-\frac{N}{2}}^{-\frac{M}{2}-1} q_m^\dagger |0\rangle, \qquad (B1)$$

with $N_n = 0, 1$ being the occupancy of correlated orbital $q_n^\dagger$, the summation restricted to occupations such that $\sum_{n=-M/2}^{M/2} N_n = M/2$ at half filling, and $\Psi(N_{-\frac{M}{2}}, \ldots, N_{\frac{M}{2}})$ being the complete wave function in the correlated subspace.

We then split the full Hamiltonian between the correlated and uncorrelated sectors as $\mathcal{H} = \mathcal{H}_{\text{corr}} + \mathcal{H}_{\text{mix}} + \mathcal{H}_{\text{uncorr}}$. We label the correlated orbitals with roman indices, such as $q_n^\dagger$ with $n = -M/2, \ldots, -1, 1, \ldots, M/2$, and
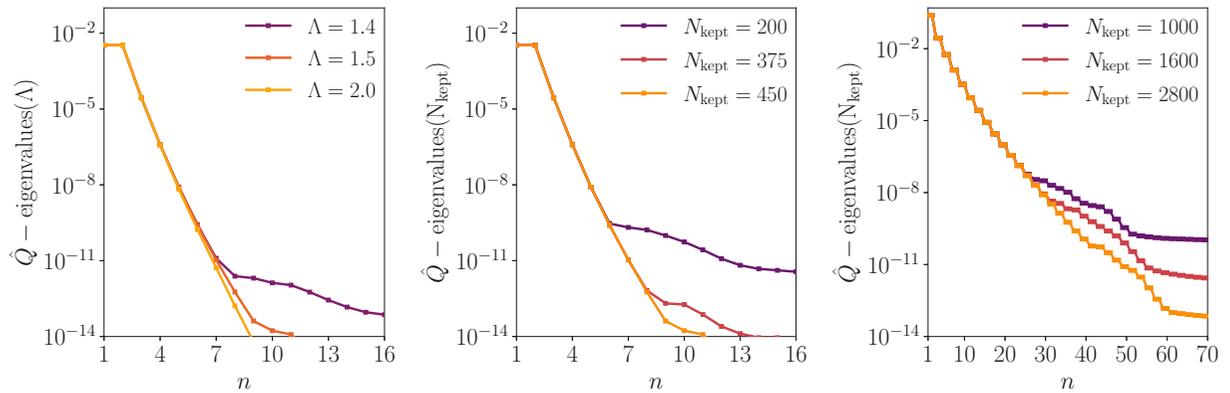
FIG. 9. (left) IRLM $\hat{Q}$ spectrum for $U = 0.5$ and $N_{\text{kept}} = 450$, for $\Lambda = 1.4, 1.5, 2.0$, showing robustness of the exponential decay in the thermodynamic limit. (center) IRLM $\hat{Q}$ spectrum as a function of N_{kept} for $\Lambda = 1.5$, displaying typical truncation errors of the NRG, and their disappearance when increasing the number of kept states. (right) SIAM $\hat{Q}$ spectrum versus N_{kept}, for $\Gamma = 0.01D$, $U = 0.2D = 20\Gamma$, and $\Lambda = 2.0$.
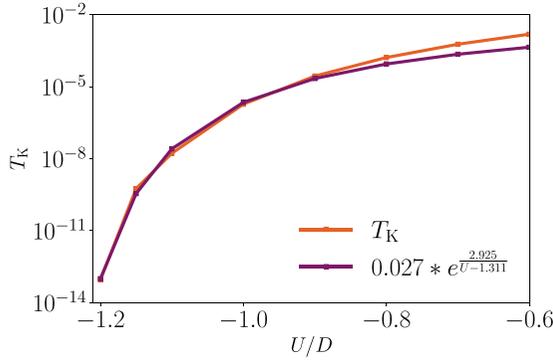
FIG. 10. Kondo temperature of the IRLM as a function of interaction U computed by NRG with Wilson discretization parameter $\Lambda = 2$ and chains of length up to $N = 110$.

uncorrelated orbitals with greek indices, such as $q_\alpha^\dagger$ with $\alpha = -N/2, \ldots, -M/2 - 1, M/2 + 1, \ldots, N/2$. The various terms read

$$\mathcal{H}_{\text{corr}} = \sum_{n,m} t_{nm} q_n^\dagger q_m + \sum_{n,m,p,q} U_{nmpq} \, q_n^\dagger q_m^\dagger q_p q_q,$$

$$\mathcal{H}_{\text{mix}} = \sum_{n,m} \sum_{\alpha,\beta} (U_{n,\alpha,m,\beta} \, q_n^\dagger q_\alpha^\dagger q_m q_\beta$$

$$+ U_{n,\alpha,\beta,m} \, q_n^\dagger q_\alpha^\dagger q_\beta q_m$$

$$+ U_{\alpha,n,m,\beta} \, q_\alpha^\dagger q_n^\dagger q_m q_\beta$$

$$+ U_{\alpha,n,\beta,m} \, q_\alpha^\dagger q_n^\dagger q_\beta q_m) + \mathcal{H}_{\text{odd}},$$

$$\mathcal{H}_{\text{uncorr}} = \sum_{\alpha,\beta} t_{\alpha\beta} q_\alpha^\dagger q_\beta + \sum_{\alpha,\beta,\gamma,\delta} U_{\alpha\beta\gamma\delta} \, q_\alpha^\dagger q_\beta^\dagger q_\gamma q_\delta, \quad \text{(B2)}$$

where $\mathcal{H}_{\text{odd}}$ contains odd terms in the uncorrelated orbitals, such as the hopping term $q_\alpha^\dagger q_n$ mixing both sectors, or interaction terms of the form $q_\alpha^\dagger q_n^\dagger q_m q_p$. The terms in $\mathcal{H}_{\text{odd}}$ vanish once we project the Hamiltonian in the family of states of the form (B1). The resulting effective few-body Hamiltonian reads

$$\mathcal{H}_{\text{few}} = \sum_{n,m} t_{nm} q_n^\dagger q_m + \sum_{n,m,p,q} U_{nmpq} \, q_n^\dagger q_m^\dagger q_p q_q$$

$$+ \sum_{n,m} \sum_\alpha q_n^\dagger q_m n_\alpha (-U_{n,\alpha,m,\alpha} + U_{n,\alpha,\alpha,m}$$

$$+ U_{\alpha,n,m,\alpha} - U_{\alpha,n,\alpha,m})$$

$$+ \sum_\alpha t_{\alpha\alpha} n_\alpha + \sum_{\alpha \neq \beta} (U_{\alpha\beta\beta\alpha} - U_{\alpha\beta\alpha\beta}) n_\alpha n_\beta, \quad \text{(B3)}$$

where n_α is the occupancy of the uncorrelated orbitals in the wave function (B1), namely, $n_\alpha = 1$ for $\alpha < -M/2$ and $n_\alpha = 0$ for $\alpha > M/2$. We note that projecting $\mathcal{H}_{\text{mix}}$ generates a renormalization of the hopping term $q_n^\dagger q_m$ within the correlated sector (the last term under the parentheses in the first line of the equation above). The projection of $\mathcal{H}_{\text{uncorr}}$ provides only a constant contribution to the Hamiltonian (second line of the equation above). The ground-state energy of the initial many-body Hamiltonian $\mathcal{H}$ is obtained by exact diagonalization of $\mathcal{H}_{\text{few}}$ in the few-body correlated sector.

APPENDIX C: EXTRACTION OF KONDO TEMPERATURE

For the IRLM, we take the following definition for the Kondo temperature:

$$T_K = \frac{1}{4\chi}, \quad \text{(C1)}$$

$$\chi = \lim_{\epsilon_d \to 0} \frac{\mathrm{d}}{\mathrm{d}\epsilon_d} \langle d^\dagger d \rangle, \quad \text{(C2)}$$

upon adding to the IRLM Hamiltonian a local potential on the d level, namely, a term $\epsilon_d d^\dagger d$. This is equivalent to the standard definition [31] for the Kondo model in terms of the magnetic susceptibility of the impurity spin. The resulting Kondo T_K temperature as a function of interaction U is given in Fig. 10. A fit of the essential singularity at the critical point allows us to determine the critical value $U_c \simeq -1.3$. We also recover our previous estimate $T_K/D \simeq 10^{-13}$ at $U = -1.2$ shown previously in Fig. 8.

[1] H. R. Krishna-Murthy, J. W. Wilkins, and K. G. Wilson, Renormalization-group approach to the Anderson model of dilute magnetic alloys. I. static properties for the symmetric case, Phys. Rev. B **21**, 1003 (1980).

[2] S. R. White, Density Matrix Formulation for Quantum Renormalization Groups, Phys. Rev. Lett. **69**, 2863 (1992).

[3] E. Gull, A. J. Millis, A. I. Lichtenstein, A. N. Rubtsov, M. Troyer, and P. Werner, Continuous-time Monte Carlo methods for quantum impurity models, Rev. Mod. Phys. **83**, 349 (2011).

[4] A. Georges, G. Kotliar, W. Krauth, and M. J. Rozenberg, Dynamical mean-field theory of strongly correlated fermion systems and the limit of infinite dimensions, Rev. Mod. Phys. **68**, 13 (1996).

[5] J. Eisert, M. Cramer, and M. B. Plenio, Colloquium: Area laws for the entanglement entropy, Rev. Mod. Phys. **82**, 277 (2010).

[6] S. Östlund and S. Rommer, Thermodynamic Limit of Density Matrix Renormalization, Phys. Rev. Lett. **75**, 3537 (1995).

[7] J. Dukelsky, M. A. Martín-Delgado, T. Nishino, and G. Sierra, Equivalence of the variational matrix product method and the density matrix renormalization group applied to spin chains, Europhys. Lett. **43**, 457 (1998).

[8] G. Vidal, Efficient Classical Simulation of Slightly Entangled Quantum Computations, Phys. Rev. Lett. **91**, 147902 (2003).

[9] U. Schollwöck, The density-matrix renormalization group in the age of matrix product states, Ann. Phys. (NY) **326**, 96 (2011).

[10] D. A. Abanin, E. Altman, I. Bloch, and M. Serbyn, Colloquium: Many-body localization, thermalization, and entanglement, Rev. Mod. Phys. **91**, 021001 (2019).

[11] A. C. Hewson, *The Kondo Problem to Heavy Fermions* (Cambridge University Press, Cambridge, New York, 1993).

[12] R. Bulla, T. A. Costi, afnd T. Pruschke, Numerical renormalization group method for quantum impurity systems, Rev. Mod. Phys. **80**, 395 (2008).

[13] V. Barzykin and I. Affleck, The Kondo Screening Cloud: What Can We Learn from Perturbation Theory? Phys. Rev. Lett. **76**, 4959 (1996).

[14] J. Park, S. S. B. Lee, Y. Oreg, and H.-S. Sim, How to Directly Measure a Kondo Cloud's Length, Phys. Rev. Lett. **110**, 246603 (2013).

[15] G. Barcza, K. Bauerbach, F. Eickhoff, F. B. Anders, F. Gebhard, and O. Legeza, Symmetric single-impurity Kondo model on a tight-binding chain: Comparison of analytical and numerical ground-state approaches, Phys. Rev. B **101**, 075132 (2020).

[16] I. V. Borzenets, J. Shim, J. C. H. Chen, A. Ludwig, A. D. Wieck, S. Tarucha, H. S. Sim, and M. Yamamoto, Observation of the Kondo screening cloud, Nature (London) **579**, 210 (2020).

[17] C. Yang and A. E. Feiguin, Unveiling the internal entanglement structure of the Kondo singlet, Phys. Rev. B **95**, 115106 (2017).

[18] R. Zheng, R. He, and Z. Lu, Natural orbitals renormalization group approach to a Kondo singlet, Sci. China: Phys., Mech. Astron. **63**, 297411 (2020).

[19] R.-Q. He and Z.-Y. Lu, Quantum renormalization groups based on natural orbitals, Phys. Rev. B **89**, 085108 (2014).

[20] Y. Lu, M. Höppner, O. Gunnarsson, and M. W. Haverkort, Efficient real-frequency solver for dynamical mean-field theory, Phys. Rev. B **90**, 085102 (2014).

[21] M. T. Fishman and S. R. White, Compression of correlation matrices and an efficient method for forming matrix product states of fermionic Gaussian states, Phys. Rev. B **92**, 075132 (2015).

[22] P. E. M. Siegbahn, J. Almlöf, A. Heiberg, and B. O. Roos, The complete active space SCF (CASSCF) method in a Newton–Raphson formulation with application to the HNO molecule, J. Chem. Phys. **74**, 2384 (1981).

[23] P. B. Vigman and A. M. Finkel'shtein, Resonant-level model in the Kondo problem, Sov. Phys. JETP **48**, 102 (1978).

[24] T. Giamarchi, *Quantum Physics in One Dimension* (Oxford University Press, New York, 2004).

[25] A. O. Gogolin, A. A. Nersesyan, and A. M. Tsvelik, *Bosonization and Strongly Correlated Systems* (Cambridge University Press, Cambridge, 2004).

[26] U. Weiss, *Quantum Dissipative Systems*, 4th ed. (World Scientific, Singapore, 2012).

[27] F. Guinea, V. Hakim, and A. Muramatsu, Bosonization of a two-level system with dissipation, Phys. Rev. B **32**, 4410 (1985).

[28] G. Zaránd and J. von Delft, Analytical calculation of the finite-size crossover spectrum of the anisotropic two-channel Kondo model, Phys. Rev. B **61**, 6918 (2000).

[29] H. T. M. Nghiem, D. M. Kennes, C. Klöckner, V. Meden, and T. A. Costi, Ohmic two-state system from the perspective of the interacting resonant level model: Thermodynamics and transient dynamics, Phys. Rev. B **93**, 165130 (2016).

[30] Z. Blunden-Codd, S. Bera, B. Bruognolo, N.-O. Linden, A. W. Chin, J. von Delft, A. Nazir, and S. Florens, Anatomy of quantum critical wave functions in dissipative impurity problems, Phys. Rev. B **95**, 085104 (2017).

[31] M. Hanl and A. Weichselbaum, Local susceptibility and Kondo scaling in the presence of finite bandwidth, Phys. Rev. B **89**, 075130 (2014).